JOURNAL OF CHEMICAL INFORMATION AND MODELING

Article

pubs.acs.org/jcim

Pharmacophore Modeling, Virtual Screening, and *in Vitro* Testing Reveal Haloperidol, Eprazinone, and Fenbutrazate as Neurokinin Receptors Ligands

Yvonne Krautscheid,[†] Carl Johann Åke Senning,[‡] Simone B. Sartori,[§] Nicolas Singewald,[§] Daniela Schuster,*[,‡] and Hermann Stuppner[†]

[†]Institute of Pharmacy/Pharmacognosy, [‡]Institute of Pharmacy/Pharmaceutical Chemistry/CAMD Group, [§]Institute of Pharmacy/Pharmacology and Toxicology, University of Innsbruck and Center for Molecular Biosciences Innsbruck (CMBI), Center for Chemistry and Biomedicine (CCB), Innrain 80-82, A-6020 Innsbruck, Austria

ABSTRACT: Neurokinin receptors (NKRs) have been shown to be involved in many physiological processes, rendering them promising novel drug targets, but also making them the possible cause for side effects of several drugs. Aiming to answer the question whether the binding to NKRs could have a share in the side effects or even the desired effects of already licensed drugs, we generated a set of ligand-based common feature pharmacophore models based on the structural information about subtype-selective and nonselective NKR antagonists and screened an in-house database mainly composed of licensed drugs. The prospective pharmacological investigations of the virtual hits haloperidol, eprazinone, and fenbutrazate confirmed them to be NKR ligands in vitro. By the identification of licensed drugs as so far unknown NKR ligands, this study contributes to establishing an activity profile of the investigated compounds and confirms the presented pharmacophore models as useful tools for this purpose.

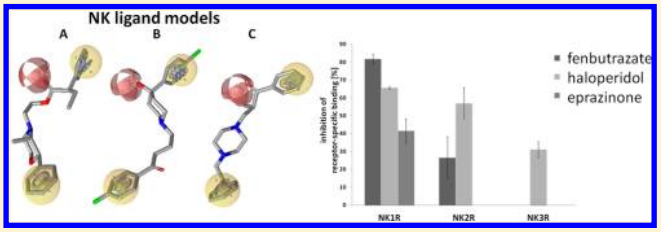

INTRODUCTION

Neurokinin receptors 1, 2, and 3 (NK_1R, NK_2R, NK_3R) belong to the family of rhodopsin-like, membrane-bound G protein coupled receptors (GPCRs). They consist of seven transmembrane domains (TM 1−7) connected over intra- and extracellular loops and therefore are classified as 7-TM-receptors.[1] Whereas the NK_2R is primarily located in peripheral tissues and has been found only in some distinct brain areas such as the hippocampus, parts of the thalamus, the nucleus accumbens, the lateral septum, and some cortical areas, the NK_3R is mainly found in the central nervous system (CNS).[2] The NK_1R is the most prevalent NKR and can be detected in the CNS and also in many peripheral cell types.[1,2] Additionally to tissues where NK_2R is expressed, Pinto et al. could detect NK_1R mRNA in thyroid gland cells, in thymus cells, and in bone marrow.[3] Because of this broad distribution, NKRs seem to be promising targets for the treatment of many diseases including asthma,[4,5] schizophrenia, depression, and anxiety disorders.[2] On the other hand, this broad expression may also cause numerous side effects of drugs, which, in addition to their main target structure, also bind to NKRs. The endogenous NKR ligands substance P (SP), neurokinin A (NKA), and neurokinin B (NKB) (Chart 1) are able to activate all three NKRs, though to different extents.[2] Specifically, SP has a preference to the NK_1R, NKA to the NK_2R, and NKB to the NK_3R. Until recently, the aim of several pharmaceutical companies has been the development of selective NKR antagonists. However, NK_1R antagonists did not show the expected effect in pain treatment,[6] and also clinical phase II and phase III studies investigating the efficacy of selective NK_2R and NK_3R antagonists have been discontinued. In 2009, Sanofi-Aventis announced the termination of clinical trials for the selective NK_2R antagonist saredutant in the treatment of depression and anxiety disorders.[7] Similarly, several NK_3R antagonists have been developed for the treatment of depression and for schizophrenia, but, again, clinical studies on selective NK_3R antagonists for psychiatric conditions were stopped.[8] So far, the only FDA-approved NKR antagonist is the NK_1R antagonist aprepitant (and its prodrug fosaprepitant; Chart 1), which is indicated against chemotherapy-induced emesis (trade names Emend and Ivemend). One reason for the disappointing results in clinical studies may be the development of subtype-selective NKR-targeting compounds on the basis of their activity data obtained in *in vitro* and *in vivo* tests on tissues and receptors from rodents. Due to species differences, both in amino acid sequence of the receptors and their tissue distribution, activity profiles of compounds acting on NKRs were found to be inconsistent.[1] Leffler et al.[9] defined the group of human, gerbil, and guinea pig receptors to show a similar response to the treatment with NKR antagonists and also detected clearly different activity data at rat NKRs. The unsatisfactory results of subtype receptor-selective compounds in clinical trials shifted the research efforts toward nonselective NKR antagonists favoring the antagonism of more than one NKR in accordance with the activity profiles of the endogenous

Received: February 20, 2014

   dx.doi.org/10.1021/ci500106z | *J. Chem. Inf. Model.* XXXX, XXX, XXX−XXX

Chart 1. Structures of Endogenous NKR Ligands and Marketed NK_1R Antagonists

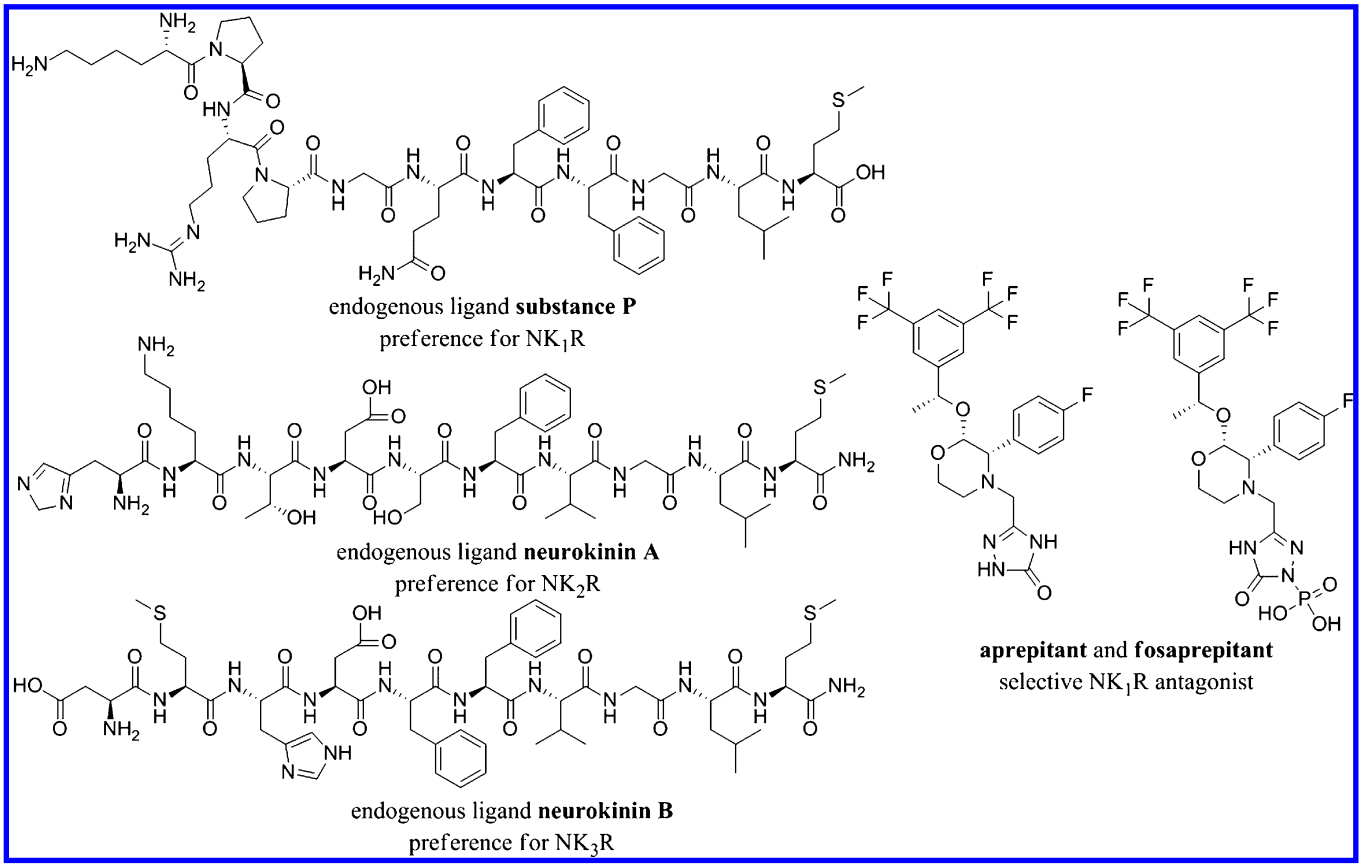

ligands SP, NKA, and NKB. For example, targeting the treatment of schizophrenia, Hoffmann−La Roche proceeded to investigate dual NK_1R-/NK_3R-antagonists,[10] while Novartis 2011 concentrated on the development of compounds binding to all three receptors.[11]

Since GPCRs are located in membranes and are therefore difficult to crystallize, so far neither crystal structures of the receptors themselves nor of the ligand-bound NKRs are available. Therefore, the exact binding sites for endogenous ligands and xenobiotics are not known. Gether et al.[12] reported different binding sites for SP and for a nonpeptide NK_1R antagonist, at the NK_1R of the rat (rNK_1R). By exchange of corresponding segments between rNK_1R and rNK_3R, they found TM5, TM6, and the adjacent part of the extracellular loop 2 of rNK_1R, not to be important for the binding of SP but for the binding of a nonpeptide antagonist to the rNK_1R. The binding site of nonpeptide antagonists at the human NK_1R was reported to be located in the region of Gln165 in TM 4 together with residues of TM 5, 6, and 7.[13] Similarly, several binding sites in the TM regions of NK_2R have been proposed for nonpeptide NK_2R antagonists. To get an idea of possible receptor-bound conformations of NKR ligands, ligand-based pharmacophore modeling and homology modeling studies based on bovine rhodopsin have been employed.[14] Chandrashekaran et al.[15] published a rhodopsin-based homology model of the NK_2R-peptide agonist binding site, and Ganjiwale et al.[16] presented a rhodopsin-based NK_3R homology model, in which they docked an NMR-derived NKB conformation. Poulsen et al.[17] presented a NK_2R antagonist pharmacophore model based on five structurally diverse compounds and consisting of three hydrophobic features (HPF) and one hydrogen bond donor (HBD). They defined two aromatic rings (ARs) linked by a hydrogen bond acceptor (HBA) as the head and one ARF as the tail of the molecules in their NKR antagonist data set. According to their results, the head and the tail part were required for NK_2R affinity, while for NK_1R affinity only the head was necessary. Further, they mentioned a "generally accepted" NK_1R pharmacophore model consisting of two ARs in a tilted arrangement connected by an HBA. Subsequently, the same group published two other NKR antagonist models consisting of three HPFs, three HBAs, and one HBD. Additionally, they extended their previously published NK_2R model by another HBA. For validation purposes, they also constructed rhodopsin-based homology models for all three NKRs. Finally, compounds fitting to one of the models were docked into the receptor models.[18] Recently, Di Fabio et al.[19] described an NK_1R pharmacophore, based on the structural information of 10 NK_1R antagonists from six structural classes, including orvepitant. This model consists of two HPFs, one ARF, and one HBAF. Although these models provided valuable insights into ligand properties of NKR antagonists, they have so far not been experimentally validated.

Given the species-specific differences of NKRs, and failure of several subtype-specific compounds in clinical trials, new hopes are now given to nonselective dual and/or triple NKR ligands with novel lead structures. We therefore generated NKR ligand models based on human and guinea pig data combining subtype-selective and nonselective compounds. The developed models were used to screen an in-house database including marketed drugs. Selected compounds were tested *in vitro*, thereby validating our hypotheses and giving starting points for lead development and drug repurposing.

dx.doi.org/10.1021/ci500106z | *J. Chem. Inf. Model.* XXXX, XXX, XXX−XXX

Chart 2. Structures of NKR Ligands, Which Served As Training- and Test-Set Compounds, Grouped by Structural Similarity and NKR-Binding Affinity (Table 1)

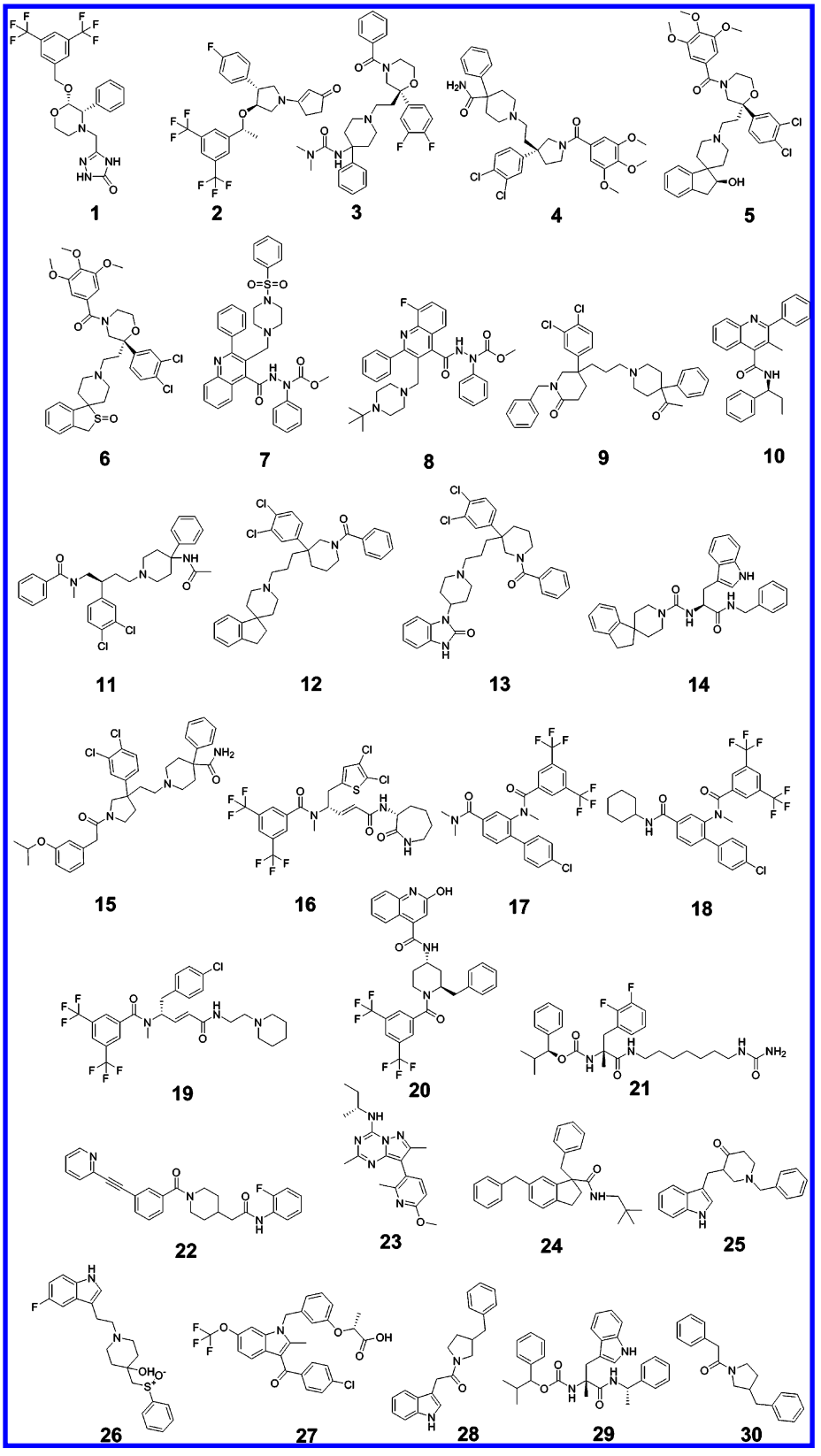

dx.doi.org/10.1021/ci500106z | J. Chem. Inf. Model. XXXX, XXX, XXX−XXX

MATERIALS AND METHODS

Data Sets. All data sets were calculated as 3D multiconformational databases using OMEGA[20−22] as incorporated in LigandScout 3.02.[23]

NKR Ligands from Literature. For the selection of NKR ligands for the training and test sets, data obtained from assays using human or guinea pig NKRs were considered. Selective and nonselective compounds of NKR subtypes were combined for the modeling. Information on chemical structures and bioactivities of compounds selected for this study was extracted from the ChEMBL database, version 10.[24] ChEMBL-listed data were filtered for small synthetic molecules, high to moderate activity in radioligand binding assays (IC_{50} <10 μM), and low conformational flexibility. Listed data were checked in the original literature for correctness, and finally, 30 diverse structures (Chart 2) were transformed into conformational models using OMEGA[20−22] as implemented in LigandScout 3.02,[23] allowing a maximum of up to 500 conformers per molecule (BEST settings).

Decoy Database. Because a set of experimentally reported NKR-inactive compounds for model evaluation was not available, a decoy set was extracted from the ChEMBL database,[24] and compounds with annotated activity on any of the NKRs were discarded. The decoy compounds should show similar physicochemical properties compared to the active NKR ligands from the literature. Therefore, these parameters were calculated from the active ligand data set using Accelrys Discovery Studio version 2.5.[25] The active molecules had a molecular weight ranging from 475 to 634, a calculated logarithm of 1-octanol/water partition coefficient (clogP) from 4 to 7, ≥ 5 rotatable bonds, ≥ 3 hydrogen-bond acceptors, and ≤3 hydrogen-bond donors. More than 61 000 database entries fulfilled these criteria. To limit the calculation and screening time with the decoy set, the decoy database size was limited to 3000 entries. For this purpose, clusters of structurally diverse compounds were built using FCFP4 fingerprint-based clustering as implemented in Accelrys Discovery Studio.[25] For each decoy molecule, a maximum of 25 conformers was calculated using OMEGA[20−22] (FAST settings) as implemented in LigandScout 3.02.[23] The final decoy database consisted of 2981 compounds, because conformation generation failed in 19 cases.

In-House Database. The in-house database of the Pharmaceutical Chemistry, Pharmacognosy, and Pharmaceutical Technology groups at the University of Innsbruck contains 2638 licensed drugs, chemically synthesized compounds (intermediates, reagents), and natural products. This database was used to select readily available virtual hits for biological evaluation. The conformational models of the in-house compounds were calculated using OMEGA[20−22] as implemented in LigandScout 3.02[23] and allowing a maximum of 100 conformers per molecule.

Drugmatrix Database. The Drugmatrix database from the U.S. Department of Health and Human Services, National Toxicology Program, is a freely available data set of 830 unique drugs and bioactive compounds, which have been experimentally evaluated against 132 drug targets (https://ntp.niehs.nih.gov/drugmatrix/index.html). For each compound and target pair, the IC_{50} or K_I value is reported. If no activity was observed up to a specific compound concentration (usually 10 μM), the compound is classified as inactive. The compound structures and biological data can be accessed via the ChEMBL database.[24] Unfortunately, the Drugmatrix data set does not contain data on NK_3R activity. Of the 830 compounds, five are reported as NK_1R antagonists and 42 as NK_2R antagonists with IC_{50}'s in the low micromolar ranges. For model quality assessment, the Drugmatrix is an invaluable resource. It provides data on hundreds of chemically diverse, experimentally confirmed, inactive molecules for all tested targets. Using this data set, an accurate determination of the false positive hit rates of models can be performed. We downloaded the Drugmatrix compounds as an sd file from ChEMBL version 18 and converted the structures into a 3D multiconformational database using OMEGA[20−22] incorporated in LigandScout 3.02.[23] For the database generation, FAST settings were used (max. 25 conformers per molecule).

Model Generation. The ligand-based common feature models were generated using the espresso module of LigandScout 3.02.[23] Different training set compounds were used to generate models complementing each other in their literature data hit lists. First, the algorithm ranks the training molecules according to their flexibility (number of conformations). Then, pharmacophore features (HPF, HBD, and HBA, positively ionizable (PIF) and negatively ionizable groups (NIF)) are projected on these molecules and their conformations. All conformations of the two least flexible molecules are then aligned using a feature-based molecular alignment algorithm.[26] For the best alignment solutions, common pharmacophoric features are interpolated and intermediate pharmacophore models are created. These intermediate models are then ranked using several adjustable scoring functions taking into account chemical feature overlap, steric overlap, or both. The intermediate models are then aligned to all conformations of the third molecule etc., and a new set of intermediate combined feature pharmacophores is created until all molecules of the training set have been processed. If at any stage no conformation can be found that can be matched on any intermediate solution, the process is stopped. If at least three common chemical features can be identified throughout the whole alignment and interpolation process, the feature pharmacophore combination is considered to be successful and the model is reported to the user.[27] Models can be sterically refined by adding exclusion volumes (EVs), forbidden areas for the ligand, where the binding site amino acids are supposedly located. LigandScout has the option to automatically place exclusion volumes around the best alignment model, thereby preventing large compounds from fitting the model.

Model Evaluation and Prospective Virtual Screening. The evaluation of the distinct models was performed by screening a test set of 2981 decoys and subsets of 27−28 active compounds (the compounds shown in Chart 2 excluding the training compounds for the respective model). In order to investigate the models' complementarity, the set of active structures comprised all 30 compounds. For the judgment of model quality, several metrics were applied, 1−4.[28]

$$\text{Yield of actives, Ya} = \text{TP}/n \tag{1}$$

$$\text{Sensitivity, Se} = \frac{\text{TP}}{\text{TP} + \text{FN}} \tag{2}$$

$$\text{Specificity, Sp} = \frac{\text{TN}}{\text{TN} + \text{FP}} \tag{3}$$

dx.doi.org/10.1021/ci500106z | J. Chem. Inf. Model. XXXX, XXX, XXX−XXX

Table 1. IC_{50} Values of Training and Test Set Compounds and Hit Identification by the Distinct Models M1−M7

Cpd	IC_{50}[a] NK_1R	IC_{50}[a] NK_2R	IC_{50}[a] NK_3R	M1	M2	M3	M4	M5	M6	M7
1	0.09[36]	7[36]	150[36]					x		
2	0.11[37]	1730[37]	>3000[37]					x	x	
3	1824[b,38]	0.04[b,38]	604[b,38]			x train[c]				x
4	3[39]	8[39]	21[40]			x train				x
5	270[41]	45[41]	17[41]		x train					
6	220[42]	59[42]	11[42]							x train
7			0.72[43]	x train						x
8	>1000[43]	50[43]	4[43]					x train		x train
9	1026[44]	3.9[44]	19[44]	x train					x train	
10			15[45]	x					x train	
11	593[40]	0.44[40]	208[40]	x		x				x
12	272[44]	204[44]	2.6[44]			x			x	x
13	379[44]	7.9[44]	348[44]			x				x
14	227[46]	14[46]			x					
15	138[40]	548[40]		x	x					x
16	3.6[d,41]	17[41]						x		
17	4[d,47]	500[47]						x		
18	3[d,47]	51[47]						x		
19	10[48]	49[48]						x train		
20	10[49]		450[49]	x						
21	3000[50]		7[50]				x train			
22	640[51]	550[51]					x train			
23		4900[52]							x	
24			5200[53]						x	
25			10[54]							
26		22[55]		x	x train					
27		530[56]					x			
28	3700[57]		3500[57]	x train						
29	1400[58]		1200[58]	x					x	
30			9400[59]	x						

[a]Given in nanomolar concentrations. [b]K_I values. [c]Compound served as training compound during the model generation process. [d]Measured at bovine retina membranes; x identified compound.

$$\text{Enrichment Factor, EF} = \frac{TP/n}{A/N} \quad (4)$$

TP, true positives

n, number of actives and decoys in the hitlist

FN, false negatives

FP, false positives

A, number of all actives in database

N, number of all compounds in both databases (actives and decoys)

The maximal possible EF (EF_{max}) for the model set would be 100.4 (A = 30; N = 3011). For **M1**, it would be 111.4 (A = 27; N = 3008), and for all other models, which are based on two training structures, it would be 107.5 (A = 28; N = 3009).

The Receiver Operating Characteristic curve (ROC curve) is defined as the TP rate (active compounds correctly classified/all active compounds) plotted on the y axis versus the FP rate (inactive compounds incorrectly classified as active/all inactive compounds) plotted on the x axis.[29] The point (0,1) represents a perfect classification. A model with pronounced early enrichment represents a model of high predictive value. The area under the curve (AUC) varies between 0 and 1.

In order to identify models able to discover already known drugs and further to pick out compounds for the pharmacological model validation, our in-house database was screened. All screenings were performed considering all EVs and pharmacophore features.

Pharmacological Evaluation of Virtual Hits on NKRs. The pharmacological *in vitro* tests were performed by the company Cerep.[30] Compounds were investigated at a concentration of 25 μM in radioligand binding assays on the hNK_1R (inhibition of [^{125}I]BH-SP binding at 0.15 nM), as described by Heuillet, E.,[31] on the hNK_2R (inhibition of [^{125}I]NKA binding at 0.1 nM) as described by Aharony et al.,[32] and on the hNK_3R (inhibition of [^{125}I][MePhe7]-NKB at 0.025 nM) as described by Anthes et al.[33] The receptor-subtype-specific binding was determined by adding unspecific binding competitors, namely on the NK_1R, [Sar^9,Met(O_2)^{11}]-SP; on the NK_2R, [Nleu^{10}]-NKA (4−10); and on the NK_3R, [MePhe^7]-NKB. Additionally, all compounds were tested for their ability to antagonize NK_1R-activation-related calcium release, mediated by the agonist [Sar^9, Met(O_2)^{11}]-SP in a cell-based calcium-detecting fluorescence assay as described by Eistetter et al.[34]

RESULTS AND DISCUSSION

While selective NKR antagonists in clinical trials had rather disappointing outcomes, new hopes are now given to dual and/or triple NKR ligands for the treatment of diverse

dx.doi.org/10.1021/ci500106z | J. Chem. Inf. Model. XXXX, XXX, XXX−XXX

Table 2. Theoretical Model Evaluation Based on the Active Literature Data and Decoy Set Screening[a]

model	identified number of actives/decoys	yield of actives	sensitivity	specificity	enrichment factor (100%)	ROC/AUC	number of in-house database hits
1	7/22	0.241	0.259	0.992	26.9	0.63	25
2	2/28	0.066	0.071	0.990	7.2	0.53	26
3	3/0	1.000	0.107	1.000	107.5	0.55	0
4	1/14	0.066	0.035	0.995	7.2	0.52	1
5	5/4	0.555	0.178	0.998	59.7	0.59	0
6	5/33	0.132	0.178	0.988	14.1	0.58	25
7	7/41	0.146	0.250	0.985	15.7	0.62	99
1−7	29/139	0.173	0.966	0.953	17.3	0.97	161

[a]From the prospective screening, results of the in-house database are given.

pathologies.[10,11] We therefore aimed to develop a set of models combining NK_1R, NK_2R, and NK_3R activity, which was able to identify the majority of NKR-active compounds from our literature data set and at the same time finds as few decoys as possible. A way to achieve this goal is the generation of various models, the hit lists of which are complementary to each other.[35] Sets of two to five compounds from the literature data set (Chart 2, Table 1) were systematically combined into training sets and used for model building by LigandScout. The resulting models were evaluated by screening the active literature data set (excluding the respective training compounds) and the decoy set. Models with good retrieval of active compounds and reasonable EFs above 5 (Table 2) were kept and combined so that their hit lists showed only a small overlap. The final model set comprised seven pharmacophore models (**M1**−**M7**) (Figure 1).

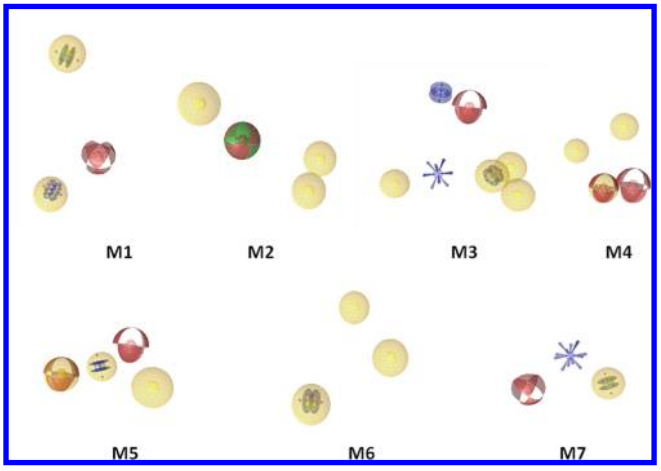

Figure 1. Illustrations of models 1−7. **M1**: 2 HPFs, both including 1 AR, 1 HBA, 42 EVs. **M2**: 3 HPFs, 1 combined HBA/HBD, 42 EVs. **M3**: 4HPFs, 2ARs, 1 PIF, 1 HBA, 50 EVs. **M4**: 2 HPFs, 1 HBA, 1 combined HPF/HBA, 50 EVs. **M5**: 2 HPFs, 1 HBA, 1 combined HPF/HBA, 1 AR, 43 EVs. **M6**: 3 HPFs, 1 including 1 AR, 45 EVs. **M7**: 1 HPF including 1 AR, 1 PIF, and 1 HBA, 25 EVs. For reasons of clarity, EVs are not shown. Chemical features are color-coded: HPF, yellow, AR, blue circles, HBA, red, PIF, blue star.

With these models (Figure 1), 29 out of 30 active compounds could be correctly identified during theoretical model evaluation (Table 2, Figure 2). The single compound not covered by any of the models was compound **25**, an indole derivative described to bind to NK_3R. Hanessian et al.[60] recently described a dual hNK_1R/hNK_3R antagonists, which was not included in our literature data set. To test if the model collection would have been able to correctly identify this new

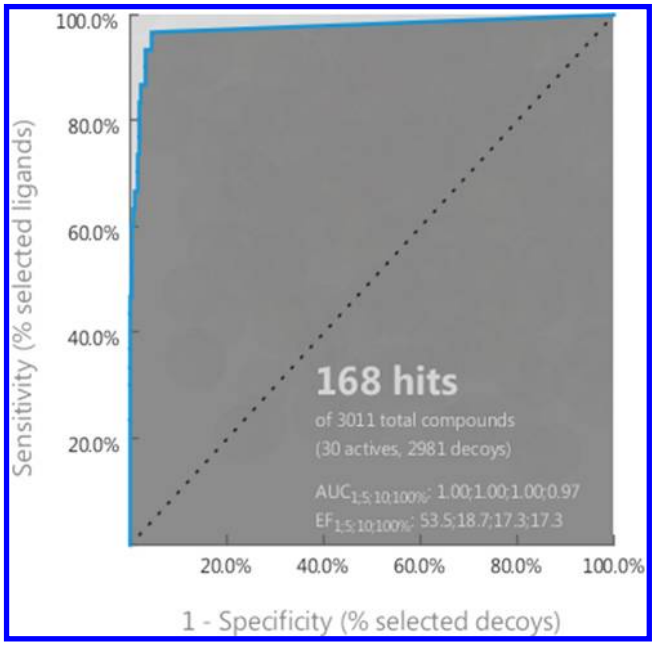

Figure 2. ROC curve and AUC resulting from the model set evaluation: 168 hits of 3011 compounds (30 actives, 2981 decoys) $AUC_{1;5;10;100\%}$: 1.00; 1.00;1.00; 0.97. $EF_{1;5;10;100\%}$: 53.5; 18.7; 17.3; 17.3. The ROC plot was calculated and visualized using LigandScout 3.02.

scaffold, compound **36** (Chart 3) was screened against all models. Indeed, **M7** recognized this compound, thereby confirming the comprehensive covering of NKR ligands by the model set.

In order to determine the correct categorization of inactive compounds, the Drugmatrix database was screened. Among the >800 experimentally evaluated compounds, five compounds were NK_1R antagonists and 42 NK_2R antagonists, respectively. The Drugmatrix, unfortunately, does not provide NK_3R activity

Chart 3. Structure of the Recently Reported Dual NK_1R/NK_3R Antagonist 36, Which Could Be Correctly Identified by M7

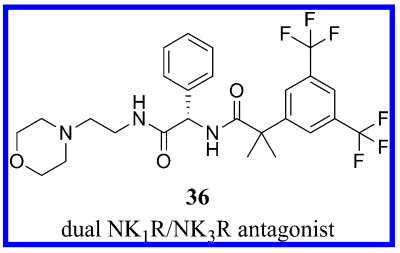

36
dual NK_1R/NK_3R antagonist

dx.doi.org/10.1021/ci500106z | J. Chem. Inf. Model. XXXX, XXX, XXX−XXX

Chart 4. Chemical Structures of Virtual Hits Selected for Experimental Validation of M1

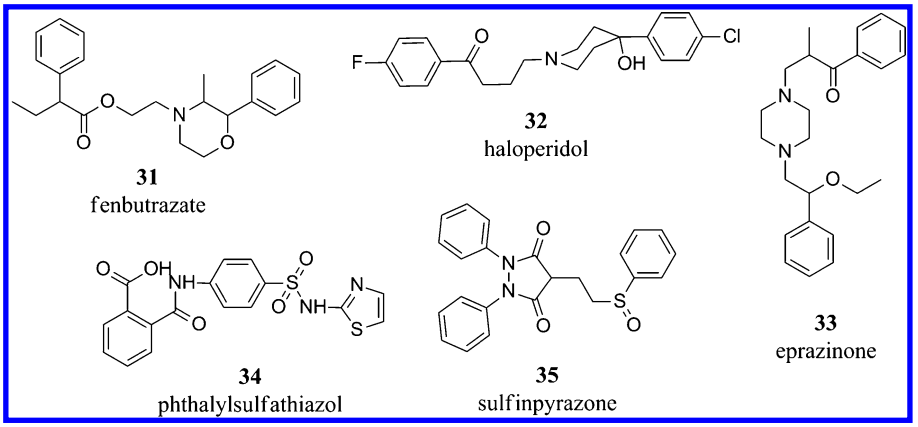

data. From the 818 compounds for which the conformer generation was successful, **M1** identified three hits (active haloperidol and two inactive hits), **M2** found haloperidol and eight inactive compounds, **M3** and **M5** found no hit, **M4** found two inactive molecules, **M6** returned five false positive hits, and **M7** identified 14 compounds, among them two active ones. These results proved a sufficient restrictivity of the generated models within a chemically diverse set of experimentally confirmed inactive compounds.

Prospective Virtual Screening. The seven generated NKR-pharmacophore models (**M1**–**M7**) were used to screen the in-house database. Out of 2638 compounds, 161 unique hits were retrieved: 25 by **M1**, 26 by **M2**, 1 by **M4**, 25 by **M6**, and 99 by **M7** (Table 2). Nine of the 25 hits of **M1** were butyrophenones, and also **M2** identified five butyrophenones, which were consensus hits of both models: haloperidol (**32**), bromperidol, moperone, trifluperidol, and benperidol. One of the additional butyrophenones identified by **M1** was the antiemetic droperidol.[61] Further antiemetic drugs selected by **M2** were the benzamides bromopride and metoclopramide, by **M6** the antihistamine meclizine, and by **M7** the phenothiazine acetophenazine. That finding is interesting in relation to the antiemetic NK_1R antagonist aprepitant. Overall, 13 of the hits derived by **M7** were neuroleptics from the class of phenothiazines, and additionally this model identified one aza-phenothiazine and spirilene, which was also identified by **M2**. Using **M7**, the antihistamine chloropyramine, the sympathomimetic fenoterol, and the anticholinergic ipratropium were identified as potential ligands to NKRs. This is of interest because these drugs are all used in the treatment of asthma, and an activation of NKRs at the airways is described to cause bronchoconstriction.[4] Another centrally available drug identified by **M7** was benserazid, a decarboxylase inhibitor used in the therapy of Morbus Parkinson.

The hit lists also comprised drugs acting on the cardiovascular system, for example the unspecific β-blocker carvedilol detected by **M1** and the ACE blocker benazepril fitting into **M1** and **M2**. In addition, **M1** selected the β-adrenergic agonists buphenine, isoxsuprine, and oxyfedrine, which was also found by **M6**. **M2** selected the β-blockers bupranolol, penbutolol, pepranolol, and toliprolol, of which bupranolol was a consensus hit of **M2** and **M7**. **M7** additionally identified lisinopril and the β-blockers alprenolol, atenolol, befunolol, betadrenol, carazolol, nadolol, oxprenolol, pamatolol, penbutolol, and practolol. **M6** selected the calcium channel blocker prenylamine.

Eight out of the 26 hits from **M2** were β-lactam antibiotics. The locally administered corticosteroid fluocortin-butyl-ester was identified by **M4**, and octinoxate, a UV filter and ingredient of sun screen, was selected by **M6**. As further antibacterial compounds, four sulfonamides were identified: phtalylsulathiazol (**34**), xyloylsulfamine, and the nonabsorbable sulfaguanol by **M2** and sulfasymazine by **M6**. Diphenoxin, a compound related to the opioid loperamide, was identified by **M1** and by **M6**, and also the uricosuric sulfinpyrazone (**35**) was identified by both of these models.

Because **M1** had the highest EF (26.9) and the most favorable active hits/decoys ratio among the models which found in-house compounds (Table 2), hits identified by this model were selected for the pharmacological model validation. Among the 25 virtual hits in the in-house db, five drugs were selected for *in vitro* testing (Chart 4): the anorectic fenbutrazate (**31**), the neuroleptic butyrophenone haloperidol (**32**), the mucolytic eprazinone (**33**), the sulfonamide phtalylsulfathiazol (**34**), and the uricosuric sulfinpyrazone (**35**).

Pharmacological Investigations. The binding assays at NK_1R, NK_2R, and NK_3R identified three out of five tested compounds as NKR antagonists. Compounds **31**, **32**, and **33** could be confirmed as NKR ligands (Figure 3A, Table 3). Furthermore, all three compounds showed an antagonistic effect at the functional NK_1R assay (Figure 3B, Table 3), which was performed because our research group is interested in the anxiolytic properties of NKR ligands, and there are especially hints for an involvement of NK_1R activation in patients suffering from anxiety disorders.[2,62]

Fenbutrazate (**31**), an anorectic drug, which is no longer marketed due to its addictive profile, had the highest NKR affinity at NK_1R and also the highest antagonistic effect at the NK_1R of all tested compounds (Figure 3A, B; Table 3). It displaced more than 80% of [^{125}I]BH-SP (K_d: 0.12 nM), from the NK_1R. Additionally, it bound to the NK_2R with low affinity. Haloperidol (**32**) was discovered to be an inhibitor of specific binding at all three NKRs, with similar and higher affinity to the NK_1R and NK_2R than to NK_3R. It displaced more than 50% of control compounds from the NK_1R ([^{125}I]BH-SP) and from the NK_2R ([^{125}I]NKA (K_d: 0.12 nM). To its main target, the dopamine D_2 receptor, haloperidol has a K_i of 0.4 nM.[63] It has to be considered that haloperidol was tested at a concentration of 25 μM. However, the fact that it binds to NKRs, in combination with the large number of butyrophenones in the virtual screening hit lists, could lead to a new interest in this structural class in the modern management of schizophrenia.

dx.doi.org/10.1021/ci500106z | J. Chem. Inf. Model. XXXX, XXX, XXX–XXX

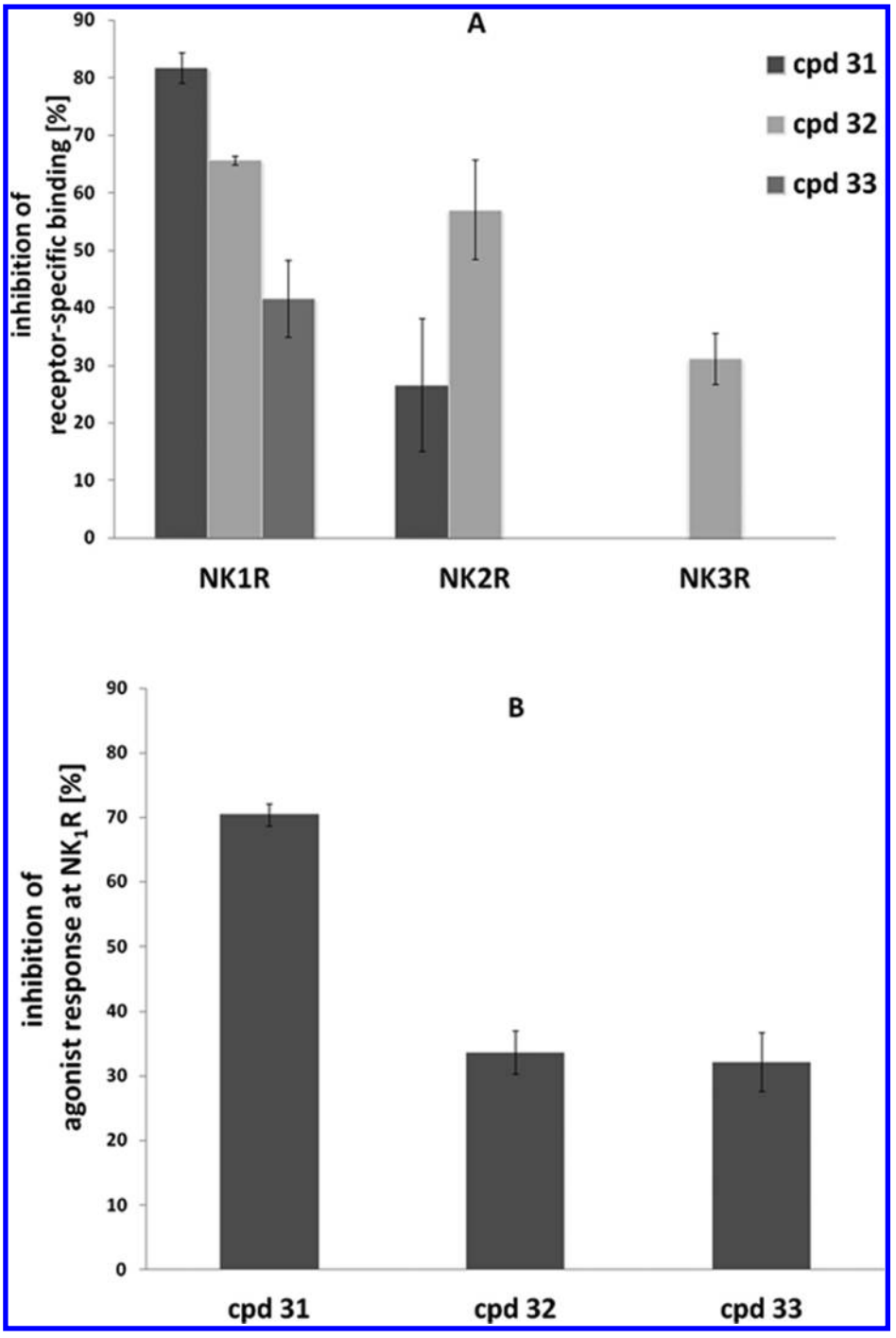

Figure 3. Results of pharmacological investigations. (A) Inhibition of specific binding at NKRs by fenbutrazate (**31**), haloperidol (**32**), and eprazinone (**33**) measured in radioligand binding assays using [^{125}I]BH-SP, [^{125}I]NKA, and [^{125}I][MePhe^{7}]-NKB as radioligands, respectively. (B) Inhibition of calcium release at the NK_1R, mediated by the agonist [Sar^{9}, Met(O_2)^{11}]-SP.

The combination of drugs affecting dopamine receptors and NKRs could represent a promising augmentation strategy in the treatment of schizophrenia. Interestingly, all of our positively tested compounds contained a keto group as HBA connected to a benzene ring as HPF (Figure 4). Therefore, it would be of interest to see if butyrophenones could serve as scaffolds to meet the requirements of combined effects on NKRs and dopamine receptors in one drug. Along these lines, a chemically modified derivative of the so-called "dirty drug" haloperidol could play a role in the progress of schizophrenia treatment. Both compounds, haloperidol and fenbutrazate, do not fit to the theory of a third HPF as a so-called tail fragment to be necessary for NK_2R affinity, which was stated by Poulsen et al.[17] Eprazinone (**33**), a mucolytic drug introduced in the 1970s, specifically displaced binding to the NK_1R (Figure 3A). Although it displayed a rather weak inhibition of [^{125}I]BH-SP-binding to NK_1R, at a concentration of 25 μM, and an antagonistic effect of about 30%, NK_1R blockade could contribute to its mucolytic activity or could even be a hint to a still unrevealed mode of action. Interestingly, Ramnarine et al. described NK_1R activation to increase mucus secretion in the trachea of ferrets.[64] Phtalylsulfathiazol (**34**), carrying a sulfone

dx.doi.org/10.1021/ci500106z | J. Chem. Inf. Model. XXXX, XXX, XXX−XXX

Table 3. Measured Values of All Five Compounds (31−35) Tested in NKR Binding Assays and the Functional Assay on NK_1R at a Concentration of 25 μM[a]

compound	inhib. of NK_1R specific binding [%]	inhib. of NK_2R specific binding [%]	inhib. of NK_3R specific binding [%]	inhib. of agonist response at NK_1R [%]
31	81.8 ± 2.7	26.7 ± 11.53	14.6 ± 2.05	70.5 ± 1.6
32	65.7 ± 0.85	57.1 ± 8.63	31.2 ± 4.45	33.7 ± 3.3
33	41.7 ± 6.72	35.9 ± 7.50	−4.9 ± 0.85	32.2 ± 4.5
34	−4.3 ± 2.8	12.7 ± 6.4	−7 ± 0.07	13.2 ± 4.6
35	−9.7 ± 7.9	11.1 ± 4.5	−9.1 ± 2.9	19.8 ± 2.7

[a]The cut-off value for considered activity was set by 25% inhibition.

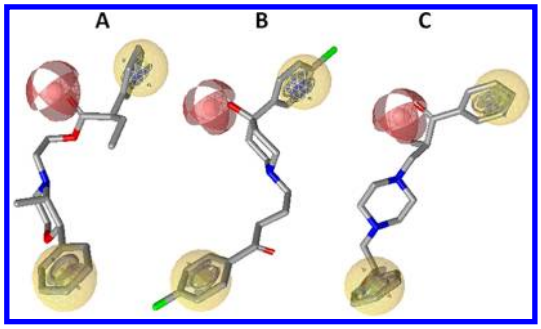

Figure 4. Pharmacologically active hits mapped into **M1**: (A) cpd **31**, (B) cpd **32**, (C) cpd **33**. In all three compounds, the HPFs (yellow) are occupied by phenyl groups, and the HBAF (red) is mapped by a keto group in the vicinity of a phenyl group.

group, and also sufinpyrazone (**35**), carrying a sulfinyl group in the immediate vicinity of a hydrophobic group, did not bind to any of the three NKRs (Table 3).

With regard to potential side effects and considering the high number of β-lactam antibiotics identified by **M2**, this scaffold should be tested for a possible effect on NKRs in future studies. Since it is highly desirable for substances used as UV filters in sun screen not to have drug-like effects on the human organism, it should also be tested if the prediction of the UV filter octinoxate can be confirmed as a NKR binding compound. Finally, drugs acting on the cardiovascular system like β-blockers were suggested during the prospective screening. Considering the hypotensive effect of NKs on the arterial blood pressure,[65] further investigations could possibly lead to a classification of the huge number of available β-blockers, in regard to an existing or absent effect on NKRs.

CONCLUSION

This study demonstrates that NKR antagonists may be unexpectedly found in currently and previously used drugs and may already contribute to their *in vivo* bioactivity profile. By prospective database screening and subsequent pharmacological validation of one NKR-pharmacophore model, it could be shown that ligand-based pharmacophore modeling is an adjuvant tool for the pharmacological profiling of already licensed drugs. The pharmacological relevance of these findings in this case study clearly depends on the potency of compounds. This study can be seen as a starting point for further pharmacological studies on the activity and potency of distinct representatives of the identified scaffolds like, e.g., butyrophenones. Although the effect of, e.g., haloperidol (**32**) was too weak to consider drug repurposing, the identification of this compound class as NKR antagonists may initiate lead optimization efforts in this field. In case of positive results for more than one member of the scaffold, the model could be adopted in accordance to structure−activity relationships. The identification of additional effects on NKRs could result in an elevated therapeutic efficacy of drug lead structures with a well-known mode of action. Additionally, the testing of further virtual hits of the presented model set could lead to a rationalization of drugs side effects caused by binding to NKRs.

AUTHOR INFORMATION

Corresponding Author

*E-mail: Daniela.Schuster@uibk.ac.at.

Notes

The authors declare no competing financial interests.

ACKNOWLEDGMENTS

This work was funded by a young investigator grant by the LFU Innsbruck (S.B.S.) and the Erika Cremer Habilitation Program (D.S.). We thank Inte:Ligand and OpenEye for providing LigandScout and OMEGA free of charge.

REFERENCES

(1) Pennefather, J. N.; Lecci, A.; Candenas, M. L.; Patak, E.; Pinto, F. M.; Maggi, C. A. Tachykinins and tachykinin receptors: a growing family. *Life Sci.* **2004**, *74*, 1445−1463.

(2) Ebner, K.; Sartori, S. B.; Singewald, N. Tachykinin receptors as therapeutic targets in stress-related disorders. *Curr. Pharm. Des.* **2009**, *15*, 1647−1674.

(3) Pinto, F. M.; Almeida, T. A.; Hernandez, M.; Devillier, P.; Advenier, C.; Candenas, M. L. mRNA expression of tachykinins and tachykinin receptors in different human tissues. *Eur. J. Pharmacol.* **2004**, *494*, 233−239.

(4) de Swert, K. O.; Joos, G. F. Extending the understanding of sensory neuropeptides. *Eur. J. Pharmacol.* **2006**, *533*, 171−181.

(5) Joos, G. F.; Germonpre, P. R.; Pauwels, R. A. Neural mechanisms in asthma. *Clin. Exp. Allergy* **2000**, *30*, 60−65.

(6) Hill, R. NK1 (substance P) receptor antagonists − why are they not analgesic in humans? *Trends Pharmacol. Sci.* **2000**, *21*, 244−246.

(7) *Sanofi-Aventis Form 20-F, Annual report pursuant to section 13 or 15(d) of the securities exchange act of 1934 for the fiscal year ended December 31, 2009*; Sanofi-Aventis: Bridgewater, NJ, 2007; p 314.

(8) Griebel, G.; Beeské, S. Is there still a future for neurokinin 3 receptor antagonists as potential drugs for the treatment of psychiatric diseases? *Pharmacol. Ther.* **2012**, *133*, 116−123.

(9) Leffler, A.; Ahlstedt, I.; Engberg, S.; Svensson, A.; Billger, M.; Öberg, L.; Bjursell, M. K.; Lindström, E.; Mentzer, B. v. Characterization of species-related differences in the pharmacology of tachykinin NK receptors 1, 2 and 3. *Biochem. Pharmacol.* **2009**, *77*, 1522−1530.

(10) Bissantz, C.; Bohnert, C.; Hoffmann, T.; Marcuz, A.; Schnider, P.; Malherbe, P. Identification of a crucial amino acid in the helix position 6.51 of human tachykinin neurokinin 1 and 3 receptors contributing to the insurmountable mode of antagonism by dual NK 1/NK 3 antagonists. *J. Med. Chem.* **2012**, *55*, 5061−5076.

(11) Zakko, S.; Barton, G.; Weber, E.; Dunger-Baldauf, C.; Rühl, A. Randomised clinical trial: the clinical effects of a novel neurokinin receptor antagonist, DNK333, in women with diarrhoea-predominant irritable bowel syndrome. *Aliment. Pharmacol. Ther.* **2011**, *33*, 1311−1321.

(12) Gether, U.; Johansen, T. E.; Snider, R. M.; Lowe, J. A.; Nakanishi, S.; Schwartz, T. W. Different binding epitopes on the NK1 receptor for substance P and a non-peptide antagonist. *Nature* **1993**, *362*, 345−348.

(13) Fong, T. M.; Yu, H.; Cascieri, M. A.; Underwood, D.; Swain, C. Interaction of glutamine 165 in the fourth transmembrane segment of the human neurokinin-1 receptor with quinuclidine antagonists. *J. Biol. Chem.* **1994**, *269*, 14957−14961.

(14) Choe, H.-W.; Park, J. H.; Kim, Y. J.; Ernst, O. P. Transmembrane signaling by GPCRs: Insight from rhodopsin and opsin structures. *Neuropharmacology* **2011**, *60*, 52−57.
(15) Chandrashekaran, I. R.; Rao, G. S.; Cowsik, S. M. Molecular modeling of the peptide agonist-binding site in a neurokinin-2 receptor. *J. Chem. Inf. Model.* **2009**, *49*, 1734−1740.
(16) Ganjiwale, A. D.; Rao, G. S.; Cowsik, S. M. Molecular modeling of neurokinin B and tachykinin NK 3 receptor complex. *J. Chem. Inf. Model.* **2011**, *51*, 2932−2938.
(17) Poulsen, A.; Liljefors, T.; Gundertofte, K.; Bjørnholm, B. A pharmacophore model for NK2 antagonist comprising compounds from several structurally diverse classes. *J. Comput.-Aided Mol. Des.* **2002**, *16*, 273−286.
(18) Poulsen, A.; Bjørnholm, B.; Gundertofte, K.; Pogozheva, I. D.; Liljefors, T. Pharmacophore and receptor models for neurokinin receptors. *J. Comput.-Aided Mol. Des.* **2003**, *17*, 765−783.
(19) Di Fabio, R.; Alvaro, G.; Braggio, S.; Carletti, R.; Gerrard, P. A.; Griffante, C.; Marchioro, C.; Pozzan, A.; Melotto, S.; Poffe, A.; Piccoli, L.; Ratti, E.; Tranquillini, E.; Trower, M.; Spada, S.; Corsi, M. Identification, biological characterization and pharmacophoric analysis of a new potent and selective NK1 receptor antagonist clinical candidate. *Bioorg. Med. Chem. Lett.* **2013**, *21*, 6264−6273.
(20) *OMEGA*, version 2.3.3; OpenEye Scientific Software, I.: Santa Fe, NM, 2009−2013.
(21) Hawkins, P. C. D.; Skillman, A. G.; Warren, G. L.; Ellingson, B. A.; Stahl, M. T. Conformer generation with OMEGA: Algorithm and validation using high quality structures from the Protein Databank and Cambridge Structural Database. *J. Chem. Inf. Model.* **2010**, *50*, 572−584.
(22) Hawkins, P. C. D.; Nicholls, A. Conformer generation with OMEGA: Learning from the data set and the analysis of failures. *J. Chem. Inf. Model.* **2012**, *52*, 2919−2936.
(23) Wolber, G.; Langer, T. LigandScout: 3-D pharmacophores derived from protein-bound ligands and their use as virtual screening filters. *J. Chem. Inf. Model.* **2005**, *45*, 160−169.
(24) Gaulton, A.; Bellis, L. J.; Bento, A. P.; Chambers, J.; Davies, M.; Hersey, A.; Light, Y.; McGlinchey, S.; Michalovich, D.; Al-Lazikani, B.; Overington, J. P. ChEMBL: a large-scale bioactivity database for drug discovery. *Nucleic Acids Res.* **2012**, *40*, D1100−D1107.
(25) *Discovery Studio 2.5*; Accelrys Inc.: San Diego, CA, 2001−2009.
(26) Wolber, G.; Dornhofer, A.; Langer, T. Efficient overlay of small molecules using 3-D pharmacophores. *J. Comput.-Aided Mol. Des.* **2006**, *20*, 773−788.
(27) *LigandScout program tutorial*; Inte:Ligand GmbH: Vienna, Austria.
(28) Triballeau, N.; Acher, F.; Brabet, I.; Pin, J.-P.; Bertrand, H.-O. Virtual screening workflow development guided by the "receiver operating characteristic" curve approach. Application to high-throughput docking on metabotropic glutamate receptor subtype 4. *J. Med. Chem.* **2005**, *48*, 2534−2547.
(29) Fawcett, T., ROC graphs: Notes and practical considerations for data mining researchers. *Technol. Rep.* **2003**, HPL-2003-4.
(30) Cerep. http://www.cerep.fr/Cerep/Users/index.asp.
(31) Heuillet, E.; Ménager, J.; Fardin, V.; Flamand, O.; Bock, M.; Garret, C.; Crespo, A.; Fallourd, A. M.; Doble, A. Characterization of a human NK 1 tachykinin receptor in the astrocytoma cell line U 373 MG. *J. Neurochem.* **1993**, *60*, 868−876.
(32) Aharony, D.; Little, J.; Powell, S.; Hopkins, B.; Bundell, K. R.; McPheat, W. L.; Gordon, R. D.; Hassall, G.; Hockney, R.; Griffin, R. Pharmacological characterization of cloned human NK-2 (neurokinin A) receptor expressed in a baculovirus/Sf-21 insect cell system. *Mol. Pharmacol.* **1993**, *44*, 356−363.
(33) Anthes, J. C.; Chapman, R. W.; Richsrd, C.; Eckel, S.; Corboz, M.; Hey, J. A.; Fernandez, X.; Greenfeder, S.; McLeod, R.; Sehring, S.; Rizzo, C.; Crawley, Y.; Shih, N. Y.; Piwinski, J.; Reichard, G.; Ting, P.; Carruthers, N.; Cuss, F. M.; Billah, M.; Kreutner, W.; Egan, R. W. SCH 206272: A potent, orally active tachykinin NK(1) NK(2) and NK(3) receptor antagonist. *Eur. J. Pharmacol.* **2002**, *450*, 191−202.
(34) Eistetter, H. R.; Mills, A.; Brewster, R.; Alouani, S.; Rambosson, C.; Kawashima, E. Functional characterization of neurokinin-1 receptors on human U373MG astrocytoma cells. *Glia* **1992**, *6*, 89−95.
(35) Schuster, D.; Waltenberger, B.; Kirchmair, J.; Distinto, S.; Markt, P.; Stuppner, H.; Rollinger, J. M.; Wolber, G. Predicting cyclooxygenase inhibition by three-dimensional pharmacophoric profiling. Part I: Model generation, validation and applicability in ethnopharmacology. *Mol. Inf.* **2010**, *29*, 75−86.
(36) Hale, J. J.; Mills, S. G.; MaCcoss, M.; Shah, S. K.; Qi, H.; Mathre, D. J.; Cascieri, M. A.; Sadowski, S.; Strader, C. D.; MacIntyre, D. E.; Metzger, J. M. 2(S)-((3,5-Bis(trifluoromethyl)benzyl)- oxy)-3(S)-phenyl-4-((3-oxo-1,2,4-triazol- 5-yl)methyl)morpholine (1): A potent, orally active, morpholine-based human neurokinin-1 receptor antagonist. *J. Med. Chem.* **1996**, *39*, 1760−1762.
(37) Lin, P.; Chang, L.; DeVita, R. J.; Young, J. R.; Eid, R.; Tong, X.; Zheng, S.; Ball, R. G.; Tsou, N. N.; Chicchi, G. G.; Kurtz, M. M.; Tsao, K.-L. C.; Wheeldon, A.; Carlson, E. J.; Eng, W.; Burns, H. D.; Hargreavesd, R. J.; Mills, S. G. The discovery of potent, selective, and orally bioavailable hNK1 antagonists derived from pyrrolidine. *Bioorg. Med. Chem. Lett.* **2007**, *17*, 5191−5198.
(38) Emonds-Alt, X.; Advenier, C.; Cognon, C.; Croci, T.; Daoui, S.; Ducoux, J. P.; Landi, M.; Naline, E.; Neliat, G.; Poncelet, M.; Proietto, V.; Van Broeck, D.; Vilain, P.; Soubrié, P.; Le Fur, G.; Maffrand, J. P.; Brelière, J. C. Biochemical and pharmacological activities of SR 144190, a new potent non-peptide tachykinin NK2 receptor antagonist. *Neuropeptides* **1997**, *31*, 449−458.
(39) Maynard, G. D.; Bratton, L. D.; Kane, J. M.; Burkholder, T. P.; Santiago, B.; Stewart, K. T.; Kudlacz, E. M.; Shatzer, S. A.; Knippenberg, R. W.; Farrell, A. M.; Logan, D. E. Synthesis and SAR of 4-(1H-benzimidazole-2-carbonyl)piperidines with dual histamine H1/tachykinin NK1 receptor antagonist activity. *Bioorg. Med. Chem. Lett.* **1997**, *7*, 2819−2824.
(40) Burkholder, P. T.; Kudlacz, E. M.; Tieu-Binh, L.; Knippenberg, R. W.; Shatzer, S. A.; Maynard, G. D.; Webster, M. E.; Horgan, S. W. Identification and chemical synthesis of MDL 105,212, a non-peptide tachykinin antagonist with high affinity for NK1 and NK2 receptors. *Bioorg. Med. Chem. Lett.* **1996**, *6*, 951−956.
(41) Gerspacher, M.; La Vecchia, L.; Mah, R.; Sprecher, A. v.; Anderson, G. P.; Subramanian, N.; Hauser, K.; Bammerlin, H.; Kimmel, S.; Pawelzik, V.; Ryffel, K.; Ball, H. A. Dual neurokinin NK1/NK2 antagonists: N-[(R,R)-(E)-1-arylmethyl-3-(2-oxo-azepan-3-yl)-carbamoyl]allyl-N-methyl-3,5-bis(trifluoromethyl)benzamides and 3-[N′-3,5-bis(trifluoromethyl)benzoyl-N-arylmethyl-N′-methylhydrazino]-N-[(R)-2-oxo-azepan-3-yl]propionamides. *Bioorg. Med. Chem. Lett.* **2001**, *11*, 3081−3084.
(42) Nishi, T.; Ishibashi, K.; Takemoto, T.; Nakajima, K.; Fukazawa, T.; Iio, Y.; Itoh, K.; Mukaiyama, O.; Yamaguchi, T. Combined tachykinin receptor antagonist: synthesis and stereochemical structure−activity relationships of novel morpholine analogues. *Bioorg. Med. Chem. Lett.* **2000**, *10*, 1665−1668.
(43) Elliott, J. M.; Carling, R. W.; Chicchi, G. G.; Crawforth, J.; Hutson, P. H.; Jones, A. B.; Kelly, S.; Marwood, R.; Meneses-Lorente, G.; Mezzogori, E.; Murray, F.; Rigby, M.; Royo, I.; Russell, M. G. N.; Shaw, D.; Sohal, B.; Tsao, K. L.; Williams, B. N′,2-Diphenylquinoline-4-carbohydrazide based NK3 receptor antagonists II. *Bioorg. Med. Chem. Lett.* **2006**, *16*, 5752−5756.
(44) Harrison, T.; Korsgaard, M. P. G.; Swain, C. J.; Cascieri, M. A.; Sadowski, S.; Seabrook, G. R. High affinity, selective neurokinin 2 and neurokinin 3 receptor antagonists from a common structural template. *Bioorg. Med. Chem. Lett.* **1998**, *8*, 1343−1348.
(45) Liu, H.; Altenbach, R. J.; Carr, T. L.; Chandran, P.; Hsieh, G. C.; Lewis, L. G. R.; Manelli, A. M.; Milicic, I.; Marsh, K. C.; Miller, T. R.; Strakhova, M. I.; Vortherms, T. A.; Wakefield, B. D.; Wetter, J. M.; Witte, D. G.; Honore, P.; Esbenshade, T. A.; Brioni, J. D.; Cowart, M. D. cis-4-(Piperazin-1-yl)-5,6,7a,8,9,10,11,11a-octahydrobenzofuro[2,3-h]quinazolin-2-amine (A-987306), a new histamine H4 R antagonist that blocks pain responses against carrageenan-induced hyperalgesia. *J. Med. Chem.* **2008**, *51*, 7094−7098.

(46) Qi, H.; Shah, S. K.; Cascieri, M. A.; Sadowski, S. J.; MaCcoss, M. L-tryptophan urea amides as NK1NK2 dual antagonists. *Bioorg. Med. Chem. Lett.* **1998**, *8*, 2259−2262.
(47) Mah, R.; Gerspachera, M.; Sprecher, A. v.; Stutz, S.; Tschinke, V.; Anderson, G. P.; Bertrand, C.; Subramanian, N.; Ball, H. A. Biphenyl derivatives as novel dual NK1/NK2-receptor antagonists. *Bioorg. Med. Chem. Lett.* **2002**, *12*, 2065−2068.
(48) Morphy, R.; Rankovic, Z. Designed multiple ligands. An emerging drug discovery paradigm. *J. Med. Chem.* **2005**, *48*, 6523−6543.
(49) Ofner, S.; Hauser, K.; Schilling, W.; Vassout, A.; Veenstra, S. J. SAR OF 2-benzyl-4-aminopiperidines: CGP 49823, an orally and centrally active non-peptide NK1 antagonist. *Bioorg. Med. Chem. Lett.* **1996**, 1623−1628.
(50) Boden, P.; Eden, J. M.; Hodgson, J.; Horwell, D. C.; Pritchard, M. C.; Raphy, J.; Suman-Chauhan, N. The development of a novel series of non-peptide tachykinin NK3 receptor selective antagonists. *Bioorg. Med. Chem. Lett.* **1995**, *5*, 1773−1777.
(51) Kordik, C. P.; Luo, C.; Gutherman, M.; Vaidya, A. H.; Rosenthal, D. I.; Crooke, J. J.; McKenney, S. L.; Plata-Salaman, C. R.; Reitz, A. B. Diarylacetylene piperidinyl amides as novel anxiolytics. *Bioorg. Med. Chem. Lett.* **2006**, *16*, 3065−3067.
(52) Gilligan, P. J.; Clarke, T.; He, L.; Lelas, S.; Li, Y.-W.; Heman, K.; Fitzgerald, L.; Miller, K.; Zhang, G.; Marshall, A.; Krause, C.; McElroy, J. F.; Ward, K.; Zeller, K.; Wong, H.; Bai, S.; Saye, J.; Grossman, S.; Zaczek, R.; Arneric, S. P.; Hartig, P.; Robertson, D.; Trainor, G. Synthesis and structure−activity relationships of 8-(pyrid-3-yl)-pyrazolo[1,5- a]-1,3,5-triazines: Potent, orally bioavailable corticotropin releasing factor receptor-1 (CRF 1) antagonists. *J. Med. Chem.* **2009**, *52*, 3084−3092.
(53) Horwell, D. C.; William, H.; Ratcliffe, G.; Willems, H. The design of dipeptide helical mimetics: The synthesis and biological activity of trisubstituted indanes. *Bioorg. Med. Chem. Lett.* **1994**, *24*, 2825−2830.
(54) Horwell, D. C.; Lennon, I. C.; Roberts, E. Alternative strategies towards the identification of chemical lead compounds by rational design. *Bioorg. Med. Chem. Lett.* **1994**, *4*, 525−530.
(55) Ali, M. A.; Bhogal, N.; Fishwick, C. W. G.; Findlay, J. B. C. Spatial requirements of the antagonist binding site of the NK2 receptor. *Bioorg. Med. Chem. Lett.* **2001**, *11*, 819−822.
(56) Debenham, S. D.; Chan, A.; WaiYu Lau, F.; Liu, W.; Wood, H. B.; Lemme, K.; Colwell, L.; Habulihaz, B.; Akiyama, T. E.; Einstein, M.; Doebber, T. W.; Sharma, N.; Wang, C. F.; Wu, M.; Berger, J. P.; Meinke, P. T. Highly functionalized 7-azaindoles as selective PPARc modulators. *Bioorg. Med. Chem. Lett.* **2008**, *18*, 4798−4801.
(57) Horwell, D. C.; Naylor, D.; Willems, H. M. G. 2,3-Substituted 2-azanorbornanes as polar *β*-turn mimetics. *Bioorg. Med. Chem. Lett.* **1997**, *7*, 31−36.
(58) Boden, P.; Eden, J. M.; Hodgson, J.; Horwell, D. C.; Hughes, J.; McKnight, A. T.; Lewthwaite, R. A.; Pritchard, M. C.; Raphy, J.; Meecham, K.; Ratcliffe, G. S.; Suman-Chauhan, N.; Woodruff, G. N. Use of a dipeptide chemical library in the development of non-peptide tachykinin NK 3 receptor selective antagonists. *J. Med. Chem.* **1996**, *39*, 1664−1675.
(59) Horwell, D. C.; Howson, W.; Naylor, D.; Willems, H. M. G. The design of polar b-turn dipeptide mimetics. *Bioorg. Med. Chem. Lett.* **1995**, *5*, 1445−1450.
(60) Hanessian, S.; Babonneau, V.; Boyer, N.; La Mannoury Cour, C.; Millan, M. J.; Nanteuil, G. d. Design and synthesis of potential dual NK1/NK3 receptor antagonists. *Bioorg. Med. Chem. Lett.* **2014**, *24*, 510−514.
(61) McKeage, K.; Simpson, D.; Wagstaff, A. J. Intravenous droperidol: A review of its use in the management of postoperative nausea and vomiting. *Drugs* **2006**, *66*, 2123−2147.
(62) Herpfer, I.; Lieb, K. Substance P receptor antagonists in psychiatry: Rationale for development and therapeutic potential. *CNS Drugs* **2005**, *19*, 275−293.
(63) Sokoloff, P. G. B.; Martres, M.-P.; Bouthenet, M.-L.; Schwartz, J.-C. Molecular cloning and characterization of a novel doapmine receptor (D3) as atarget for neuroleptics. *Nature* **1990**, *347*, 147−151.
(64) Ramnarine, S. I.; Hirayama, Y.; Barnes, P. J.; Rogers, D. F. 'Sensory-efferent' neural control of mucus secretion: Characterization using tachykinin receptor antagonists in ferret trachea in vitro. *Br. J. Pharmacol.* **1994**, *113*, 1183−1190.
(65) Severini, C.; Improta, G.; Falconieri-Erspamer, G.; Salvadori, S.; Erspamer, V. The tachykinin peptide family. *Pharmacol. Rev.* **2002**, *54*, 285−322.